AD-A155 554 A STUDY OF ADHERENT OXIDE SCALES(U) UNITED TECHNOLOGIES 1/1
RESEARCH CENTER EAST HARTFORD CT J G SMEGGIL ET AL.
MAY 85 UTRC/R85-916564-1 N00014-82-C-0618

UNCLASSIFIED F/G 11/6 NL

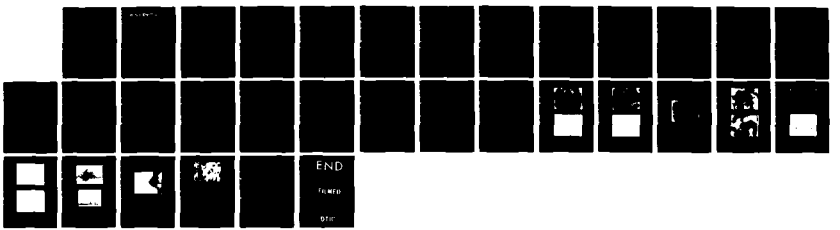

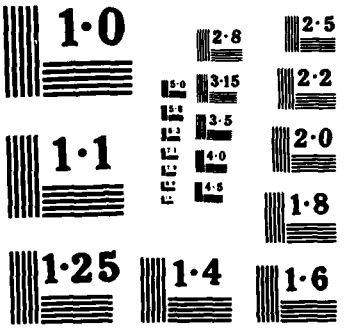

NATIONAL BUREAU OF STANDARDS
MICROCOPY RESOLUTION TEST CHART

(12)

UNITED TECHNOLOGIES RESEARCH CENTER

East Hartford, Connecticut 06108

A Study of Adherent Oxide Scales

R85-916564-1

N00014-82-C-0618

REPORTED BY J. G. Smeggil

A. W. Funkenbusch

APPROVED BY N. S. Bornstein
Chief, Materials Process Research

DATE May, 1985

A-1

NO. OF PAGES _____

COPY NO. _____

R85-916564-1

A Study of Adherent Oxide Scales

Abstract

The effects whereby minor element additions (yttrium) improve oxide scale adherence were investigated. These studies have led to the proposal of a new and different mechanism for oxide scale adherence. This new mechanism involves the effects of interfacial segregation of indigenous alloy impurities such as sulfur. Results of these studies are presented herein.

Key Words: Oxidation, Oxide Scale Formation,
Coatings, Laser-Processing,
Oxide Scale Adherence, Minor Element Effects,
Auger Electron Spectroscopy,

SUMMARY

A new mechanism to account for the beneficial effects that small additions of elements such as yttrium have on the adherence of oxide scales is proposed. Sulfur is known to be present at tramp levels (<100 ppm) within nickel and nickel-based alloys and it can segregate to metal surfaces. However, it has been disclosed here that such sulfur segregation can also markedly affect the adherence of the protective oxide scale. In the absence of elements like yttrium, such segregation effects weaken the bond between the protective scale and the substrate metal. The role of the yttrium is to interact with sulfur to form a refractory sulfide. This interaction lessens the amount of sulfur available to segregate to and concentrate at the critical scale-metal interface. The results of experiments involving Auger spectroscopy, optical, scanning electron microscopy, scanning electron microprobe and scanning transmission electron microscopy techniques in conjunction with isothermal and cyclic oxidation testing which have led us to propose this mechanism are presented.

The highlights of this period are:

- Sulfur positively identified on the surface of NiCrAl alloys.
- The concentration of sulfur on the surface of NiCrAl was more than 4-fold greater than that observed on NiCrAlY.
- Depth of sulfur layer appears to be less than 20 A thick.
- Sulfur was shown to markedly increase the rate of oxide scale spallation on NiCrAl and NiCrAlY alloys.
- The addition of yttrium to sulfur doped NiCrAl and NiCrAlY alloys restored oxide scale adherency.
- Rapid solidification processing (laser) of NiCrAl, and sulfur doped NiCrAl and NiCrAlY alloys extended the duration during which adherent oxide scales appeared to form. However, in prolonged tests, the rate of oxidation and scale spallation reverted to the prior behavior typical of the alloy.

R85-916564-1

A Study of Adherent Oxide Scales

TABLE OF CONTENTS

		PAGE
I.	INTRODUCTION	1
II.	EXPERIMENTAL MATERIALS AND PROCEDURES	3
	A. Materials	3
	B. Experimental Procedures	3
III.	RESULTS	4
	A. Auger Studies	4
	B. Cyclic Oxidation Studies	4
	C. Metallographic Studies	5
IV.	DISCUSSION	8
V.	FUTURE RESEARCH	12
VI.	ACKNOWLEDGEMENTS	12
REFERENCES	. . . . .	13
TABLES		
FIGURES		

I. INTRODUCTION

In applications requiring exposure to aggressive atmospheres at elevated temperatures, protective coatings are frequently applied to structural alloys to achieve enhanced service lifetimes. The coatings tend to form alumina rich scales and alumina is the protective scale of choice for high temperature applications since it displays: 1) limited volatility; 2) slow growth kinetics; and 3) relative chemical inertness in high temperature oxidizing environments. However, in order for alumina scales to be useful, they must adhere to the underlying alloy under thermal cycling conditions.

In the oxidation of both simple binary MAl and the ternary MCrAl alloys of interest, (in which M=Fe, Ni, Co or a combination of these elements) alumina scales readily form. However, on cooling to room temperature, exfoliation of protective alumina scales has been commonly noted. Cyclic oxidation testing merely exacerbated such exfoliation effects. To achieve scale adherency under thermal cycling conditions, it has been long known that additions of reactive elements such as yttrium (at approximately 0.1 wt.%) is highly effective (e.g., Ref. 1).

Mechanisms proposed to account for the beneficial effects of reactive element additions such as yttrium have included the following:

1. the formation of protective pegs which serve to "anchor" the scale to the substrate metal alloy (Ref. 1);

2. the prevention of vacancy coalescence at the scale-metal interface by providing alternative coalescence sites (Ref. 2);

3. the enhancement of scale plasticity by altering structure (Ref. 3);

4. the alteration or modification of scale growth processes (Ref. 4);

5. the formation of a graded oxide layer to lessen thermo-mechanical differences between the scale and the substrate metal (Ref. 5); and

6. the development of enhanced bonding forces between the scale and substrate metal through preferential segregation of the reactive element to this interface (Ref. 1).

Concerning these proposed mechanisms, the two which have been the most frequently cited involved (1) and (2) from above. However, in our prior reported studies (Refs. 6, 7), oxide pegs were rarely found at the base of scale of the strongly adherent scales formed on NiCrAl alloys to which elemental yttrium additions had been made. On the other hand, hafium-containing NiCrAl alloys similarly prepared and oxidized showed extensive oxide peg formation (Refs. 7, 8). Despite profuse oxide peg development, extensive scale exfoliation occurred in the thermal cycling of these alloys (Refs. 7,8). Hence, based on these findings, the relationship between oxide peg formation and protective scale adherency is not evident.

In regards to the mechanism number (2) above, although NiCrAl alloys (to which no reactive element additions were made) exhibited scale exfoliation, only a very few, relatively small pores were subsequently found on the metal surface juxtaposed to the absent (exfoliated) scale (Ref. 7). Hence, no relationship between pore formation and protective scale adherence effects was apparent.

Based upon experimental results which will be reported herein, previously unconsidered factors influencing oxide scale adherence effects will be disclosed. Specifically, impurity elements such as sulfur which are known to be commonly indigenously present within nickel and nickel-based alloys at tramp levels (Refs. 9-12) will be shown to have an important effect upon oxide scale-metal substrate adherence properties. By segregation effects such elements could accumulate at the critical scale-metal interface thereby weakening adherence properties. The role of the reactive element then would be to interact with tramp elements such as sulfur forming refractory phases thereby limiting the amount of sulfur which can migrate to the scale-substrate interface. Experimental results which have led us to these conclusions are presented herein.

II. EXPERIMENTAL MATERIALS AND PROCEDURES

A. Materials

Alloys were prepared using nickel and aluminum of 99.9 wt.% purity and chromium of 99.99 wt.% purity. The elemental combinations were combined, vacuum melted in alumina crucibles and poured into 2.5 cm chilled copper molds. Rods of nominally Ni-20 wt.% Cr-12 wt.% Al, which functioned as the baseline composition, were modified in the following manner: 1) no intentional minor element addition; 2) 0.1 wt.% Y; 3) 0.3 wt.% Y; 4) 0.15 wt.% Y_2S_3; 5) 0.45 wt.% Y_2S_3; 6) 0.15 wt.% Y_2S_3 and 0.1 wt.% Y; and 7) 0.45 wt.% Y_2S_3 and 0.3 wt.% Y. After casting, all rods were homogenized by heat treating in vacuum at 1200°C for 48 hours in order to reduce solidification induced compositional gradients. Analysis of the baseline alloy showed that it contained less than 50 ppm sulfur by weight.

B. Experimental Procedures

Auger studies were performed on two specimens of alloy 1 (NiCrAl) and two specimens of alloy 2 (NiCrAl + 0.1 wt.% Y). Rectangular specimens (1 X 0.1 X 0.1 cm) were electropolished in chilled perchloric acid and spot welded to a platinum wire (which was subsequently heated by electric resistance). A thermocouple spot welded to the sample was used to monitor temperature. After system evacuation to approximately 2×10^{-9} torr, one specimen of each type was argon ion sputter etched to remove surface contamination prior to heating while another specimen of each alloy was heated without prior sputtering. Specimens were heated to temperatures between 800°C and 1000°C. Surface composition was monitored as a function of time at each temperature until steady state conditions were obtained (<10 minutes). Several Auger spectra were then recorded.

Cyclic oxidation tests were conducted on all seven alloys. Two sets of experiments were conducted. In one case, specimens were cycled to 1050°C (55 minutes at test and 5 minutes at room temperature) for 1000 hours. In the other test, specimens were cycled similarly but to 1180°C. Here only three hundred hours of testing was needed to show marked differences in specimen behavior. For all cyclic oxidation tests, duplicate specimens were used; negligible differences in the mass change data were observed between the two test specimens of each alloy. Although the majority of testing involved utilized cyclic oxidation conditions, some specimens intended for metallographic studies were oxidized isothermally or cyclicly at either 1050°C or 1180°C for 100 hours.

Both as-prepared and oxidized specimens were examined by a combination of optical and, scanning electron microscopy as well as by scanning electron microprobe techniques. A scanning transmission electron microscope was used to examine and characterize precipitates formed at the scale-metal interface of mechanically stripped thermally grown scales.

III. RESULTS

A. Auger Studies

In addition to the alloying elements, high concentrations of sulfur were observed on heated specimen surfaces. The calculated surface concentration of sulfur for the two alloys (with and without preheat sputter cleaning) are shown as a function of temperature in Fig. 1. The sulfur concentrations were much higher on the NiCrAl specimen (approximately 20 at %) than on the NiCrAlY (approximately 5 at %) and increased very slightly with temperature. The preheat sputter etching step had little influence on sulfur segregation. Subsequent chemical depth profiling using argon ion sputtering showed that sulfur was present in a layer less than 20 A thick.

Hence, the Auger spectroscopy data indicated that sulfur indigenously present within the alloy did segregate to the free metral surface in the high vacuum conditions present within the Auger spectrometer. Because of this finding, metallographic and kinetic oxidation studies were conducted to discern if indeed such sulfur could influence oxidation properties by segregation to the critical protective scale-substrate alloy interface during the course of elevated temperature exposure. Hence, to elucidate such phenomena, the effects of both indigenous sulfur within the baseline alloy and sulfur intentionally added as Y_2S_3 were investigated and characterized.

B. Cyclic Oxidation Studies

The results of cyclic experiments conducted to 1050°C (55 minutes at 1050°C and 5 minutes at room temperature) are presented in terms of mass change as a function of time, i.e., number of test cycles. For the baseline alloy NiCrAl, specimen mass decreased in testing. Such mass losses indicated scale exfoliation effects were occurring during the test. These scale exfoliation effects were also visually confirmed. The addition of elemental yttrium (alloys numbered 2 and 3) prevented oxide scale exfoliation as demonstrated by small specimen mass increases. With yttrium sulfide (Y_2S_3) additions alone, severe scale exfoliation ensued resulting in large mass losses. Finally, when both elemental yttrium and the more stable yttrium sulfide were added (alloys numbered 6 and 7), good oxide scale adherence and slight mass increases were effected.

In the 1180°C cyclic oxidation test, effectively similar results were produced, Fig. 3. The baseline alloy NiCrAl (alloy numbered 1) showed mass losses almost from the inception of the test. With the addition of elemental yttrium to this baseline composition, oxide scale adherence was enhanced as indicated by the performance of alloys numbered 2 and 3. However, when yttrium was added to the baseline alloy as the sesquisulfide (Y_2S_3), oxidation resistance was severely debited. With the addition of elemental yttrium to the Y_2S_3-containing alloys, good oxide scale adherence and protective kinetics were re-engendered.

C. Metallographic Studies

Initial Alloy Microstructure and Phase Identification

The overall phase distribution of the NiCrAl alloys examined here has been well documented, (Refs. 6, 7). The principal metallic phases involved included gamma nickel solid solution, the intermetallic phase NiAl, and alpha chromium precipitates. A backscattered electron micrograph representative of this distribution has been presented along with attendant x-ray maps for aluminum and chromium, cf. Figs. 4a, 4b, and 4c.

However above and beyond the distribution of metallic phases in these materials, the distribution and composition of non-metallic phases was directly relevant to these studies. As shown in the backscattered electron micrograph shown in Fig. 4, micron and sub-micron sized low average atomic number particles randomly occurred, appearing as dark spots. Oxide inclusions were to be expected within the alloy given the use of an alumina crucible to hold the molten metal prior to casting, cf. Experimental Section above. Such expectations were confirmed by the electron microprobe, indeed finding such particles were frequently enriched in aluminum and oxygen. Additionally and more relevantly to this study, not infrequently such particles in the baseline NiCrAl alloy evidenced sulfur enrichments as presented in the x-ray map for sulfur in Fig. 4d. Indeed with a little patience, numerous such sulfur-containing particles were found randomly dispersed along with oxide particles within the alloy, Fig. 5. Although not evident in the x-ray maps contained in either Fig. 4 or 5, the sulfur-containing particles found here were enriched in aluminum and/or chromium. Based upon the experimental findings presented here, the sulfur level (<100 ppm) indigenously present in this alloy has exceeded the solubility product of some chromium- and/or aluminum-containing phase and precipitated out of solution.

In the NiCrAl alloys containing elemental yttrium additions, the distribution of metallic phases was essentially the same as that seen for the baseline alloy NiCrAl not containing yttrium, cf. Figs. 4 and 6. Examination of polished specimens soon after polishing showed many nickel yttride phases with little oxygen present. However for specimens examined several days after polishing the nickel yttride phase particles were essentially converted to an yttrium-enriched oxide phase. This was not unexpected because similar transition metal-rare earth phases have been

well known to oxidize relatively rapidly in ambient environments (Ref. 13). Additionally, many of the yttrium-enriched particles were also found to be oxygen-enriched, Fig. 5d. The oxygen-enrichments associated with the yttrium-containing particles likely derived from the alloy fabrication technique involving the use of alumina crucibles to hold the molten alloy and/or, as just pointed out, from ambient temperature oxidation of the tiny intermetallic yttride particles. This was not unexpected.

However, in the NiCrAl alloys formulated with metallic yttrium, extensive examination of several specimens with the electron microprobe revealed only a singular particle enriched in sulfur, Fig. 6f. This particle also contained both yttrium and oxygen, Fig. 6a, 6d and 6e.

With the addition of yttrium sulfide, Y_2S_3, to the NiCrAl alloy, sub-micron sized particles simultaneously enriched in both yttrium and sulfur were commonly observed, Fig. 7. In fact, no particles enriched in yttrium without a simultaneous enrichment of sulfur could be found. Additionally nickel, chromium and aluminum were excluded from these particles, i.e., as compared with matrix alloy concentrations.

Oxidized NiCrAl and NiCrAlY Specimens

Substantial - but not complete - protective scale exfoliation occurred when specimens of NiCrAl were cooled from either 1050°C or 1180°C to room temperature. Thusly, a specimen of NiCrAl isothermally oxidized at 1050°C for 100 hours with the alumina scale still partially adherent was metallographically mounted and polished. In examination by the electron microprobe in line scan mode, regions of the specimens with alumina scales still adherent showed sulfur enrichments at the scale-metal interface, Fig. 8. Despite numerous attempts using the same technique, no similar sulfur enrichments could be found using the electron microprobe at the scale-metal interface in the case of similarly tested and prepared NiCrAlY specimens. This finding did not necessarily imply that sulfur enrichments were uniquely absent at those interfaces. Rather if such enrichments were there, they were below the detection limits of the electron microprobe.

To discern more closely if indeed sulfur enrichments were to be found at the scale-metal interface, oxide scales from specimens of NiCrAl with elemental yttrium additions after 100 hours of isothermal and cyclic testing were examined by scanning transmission electron microscopy. Specifically the scales were mechanically removed, and particles present at the scale-metal interface were examined. In the case of both isothermally and cyclically tested specimens, numerous sub-micron particles were detected in the scale at this interface. However, whenever a particle was identified as having an yttrium-enrichment concomitantly a sulfur enrichment was also observed, Fig. 9. (Additionally, evidence for other indigenous impurities such as chlorine, silicon, potassium, iron and perhaps zinc and even copper were also found to be present at this crucial scale-metal interface. These elements are also likely either to be indigenous impurities in the starting materials at low levels or to be contaminants picked up during conventional alloy formulation practices as were used here. Laser-surface processed specimens similarly tested have indicated the presence of concomitant yttrium and sulfur enrichments in

discrete particles at the base of protective alumina scales. However the additional tramp element impurities found here were effectively eliminated by such surface laser melting operations as determined by a similar scanning transmission electron microscopic examination of appropriate oxide scales, (Fig. 10).

IV. DISCUSSION

Supported by data derived from both light and electron optic metallographic examination techniques, the results of both surface segregation and the cyclic oxidation studies have supported a new and a radically different mechanism for improved oxide scale adherence characteristics as effected by yttrium additions in particular and, by implication, "reactive element" additions in general (Ref. 7, 14). A similar effect has subsequently been hypothesized by others (Ref. 15).

In essence then, in the absence of reactive element additions, certainly sulfur (and possibly other impurity elements) present within the alloy at low levels (<100 ppm) can segregate to the free alloy surface when such alloys are heated within the high vacuum conditions of an Auger spectrometer. As shown in Fig. 1, yttrium additions present within the NiCrAl alloy temper such surface enrichments.

Using conventional metallurgical practices and starting materials of high purity (99.9% or better), discrete micron and sub-micron sized sulfur-enriched particles were readily found precipitated within the NiCrAl alloy. Normal scanning electron microprobe techniques easily detected these particles. Given the elevated temperature exposure in the Auger studies, it could be speculated that the source of at least some of that surface segregated sulfur could have arisen from the dissolution (or partial dissolution) of such aluminum- and/or chromium-sulfides. Such "dissolved" sulfur could then be available to transport to low energy boundaries within the alloy (Refs. 9-12). Low energy boundaries could include both alloy grain boundaries as well as the free alloy surface.

With the addition of elemental yttrium to the baseline NiCrAl alloy, the quantity of sulfur-enriched particles detectable via the scanning electron microprobe decreased markedly. The only sulfur-enriched particle found in the NiCrAl alloys modified by the addition of elemental yttrium was to be found in Fig. 6. Two plausible explanations can be suggested to account for this disparity. In the first place, the sulfur content of the alloy could have been reduced in the molten state by interaction with the elemental yttrium addition to form a refractory compound, e.g., YS. Yttrium has been reported to be an exceedingly strong sulfide former (Ref. 16). In fact, yttrium is a stronger sulfide former than either nickel, chromium, or aluminum (Refs. 16, 17). Such a refractory compound formed in the molten state may have been carried away with the slag which normally forms during such alloy processing.

In the second place, the yttrium sulfide particles could still be present within the alloy. However, despite the 1200°C annealing treatment given the alloy rods, the yttrium-sulfur particles could have retained a sub-micron size and consequently were below the limits of detectability of the electron microprobe. Even if such yttrium-sulfur containing particles were retained within the alloy, and if indeed yttrium sulfides (or oxysulfides) are indeed more stable than nickel, chromium, or aluminum sulfides, then sulfur segregation effects either to alloy grain boundaries or to a free surface would be reduced. Either of these two scenarios for the interaction between yttrium and sulfur would both be consistent with and explain both the Auger spectroscopy data of heated specimens and the

metallographic observations involving the NiCrAl and NiCrAl + elemental yttrium starting alloys.

On cooling from 1050°C after a 100 hour exposure, much of the protective scale formed on the NiCrAl alloy exfoliated as had been expected. Examination of cross-sections of the specimen where scale exfoliation had not occurred clearly revealed sulfur enrichments at the critical scale-metal interface during elevated temperature exposure, Fig. 8. Similarly examined scales formed on numerous specimens of NiCrAl alloys with elemental yttrium additions failed to show any such enrichments using scanning electron microprobe techniques. However, such sulfur enrichments were indeed there but were associated with yttrium-containing particles, (Figs. 9 and 10). Moreover to find such particles, the very high resolution powers of the scanning transmission electron microscope were required.

To determine if indeed this phenomena could more effectively be examined, yttrium sesquisulfide, Y_2S_3, additions were made to the NiCrAl baseline alloy. Here sulfur additions would be made in conjunction with the element, yttrium, which has normally been considered to be benevolent from the viewpoint of bestowing beneficial oxide scale adherence effects on the substrate alloy. However given the context of the thesis proposed so far, such yttrium additions would likely be ineffectual in promoting oxide scale adherence. This is because, based on the model presented here, such yttrium is necessary within the alloy to scavange the indigenously present sulfur within the alloy itself. With the yttrium addition made in the form of the sesquisulfide, such yttrium is already tied up and cannot benefit oxide scale adherence because of two reasons. In the first place, it cannot further scavange ingenous sulfur from the alloy constituents because it has been added here as the highest yttrium sulfide phase reported, i.e., Y_2S_3 (Refs. 18-21). Secondly, it could be speculated that the yttrium sesquisulfide addition itself could be a source of "free" sulfur for the alloy. Although the phase diagram for the yttrium-sulfur system has not been reported, the most metal-rich yttrium-sulfur phase reported is the monosulfide, i.e., YS. If, in the alloy, the sesquisulfide phase were to decompose all the way to the monosulfide, then additional "free" sulfur would be liberated:

$$Y_2S_3 \text{ ---}>> 2YS + \text{"S"}.$$

This additional librated sulfur present within the alloy would exacerbate the already poor oxide scale adherence properties of the baseline NiCrAlY alloy.

Experimentally when Y_2S_3 was added to the baseline NiCrAl alloy, discrete particles enriched in yttrium and sulfur were readily detected, Fig. 7. In cyclic oxidation, such NiCrAl alloys (numbered 4 and 5) exhibited markedly poorer oxide scale adherence properties even as compared with the baseline NiCrAl alloy (numbered 1) in Figs. 2 and 3. When elemental yttrium additions were made to the NiCrAl alloys containing Y_2S_3 (alloys numbered 6 and 7), elemental yttrium was available to react with such sulfur liberated from the Y_2S_3 thereby restoring good scale adherence, Figs. 2 and 3.

Although the emphasis here has been on the interaction of yttrium (in particular and "reactive elements" in general) with sulfur in the liquid or solid state to form stable refractory sulfides, when such reactive elements are present as oxides their role could be to provide an increased amount of oxide-metal interface thereby reducing the amount of sulfur available for segregation to the critical protective oxide-metal interface. Alternatively and more conventionally, a reaction between the oxides and sulfur toform refractory oxysulfides could also be possible. It should be noted here that, unlike both yttrium and Y_2O_3 additions which have been well known to benefit oxide scale adherence, Y_2S_3 additions were highly detrimental; the reasons for this disparity have already been discussed.

In support of the novel mechanism proposed here for oxide scale adherence effects, the strength of grain boundaries within nickel alloys has been reported to be improved analogously. In the absence of reactive elements, sulfur has been reported to segregate to and embrittle grain boundaries (Refs. 9-12). Additions of reactive elements have been shown to reduce such sulfur segregation and thereby improve grain boundary strength (Refs. 11 and 12). A close relationship exists between the elements which segregate to grain boundaries and those which segregate to exterior surfaces although differences are noted in enrichment ratios and other segregation characteristics (Ref. 22). Both surface and grain boundary segregation are driven by reduced interfacial energy and by the energy reduction achieved when a solute atom which fits poorly in a matrix lattice (due to size or electronic considerations) moves to the more open interfacial structure. Sulfur has been repeatedly observed to segregate to the exterior surfaces of nickel and nickel alloys (Refs. 8, 10, 23-27). Additionally although previous investigators have speculated on the influence of surface segregation on wetting and gas permeation (Ref. 28), the studies reported herein represent the first to relate oxide scale-metal substrate segregation effects to oxide scale adherence characteristics.

Regarding the mechanisms enumeerated in the introduction as having been proposed to account for the beneficial effects of yttrium on oxide scale adherence characteristics, it should be noted that the mechanism proposed here is essentially independent of all those in that list with one interesting exception. The last mechanism in that list suggested that preferential segregation of yttrium to the interface between the scale and the metal would effect enhanced bonding between the scale and the metal (Ref. 1). The crucial point of that mechanism is that the bond between the metal and the scale is intrinsically weak. By the segregation of yttrium to that interface, the poor bond between the scale and the metal is strengthened, perhaps through the development of some kind of very strong van der Waal's forces. On the other hand, the new mechanism which we have proposed here is the direct antithesis of that earlier one. In essence, it has been proposed here that the bond between the alumina scale and the metal substrate is intrinsically strong. However by the segregation of elements such as sulfur to that interface, bond strength between the scale and the metal has been drastically reduced.

The negative effects of sulfur segregation to the scale-metal interface have been abundantly demonstrated in this study. However, it is also to be pointed out that the precise mechanism whereby the sulfur weakens the adhesive between the scale and the substrate has not been identified. As a final consideration, it is possible that other impurities, such as were found by scanning transmission electron microscopy techniques at the base of NiCrAl alloys with yttrium, cf. Fig. 9, could also adversely affect scale adherence. (It is to be noted that laser surface processing eliminated such impurities [other than sulfur]. This elimination could have resulted from either vaporization effects or their incorporation into the oxide formed during the laser prcoessing operation.) The complex interplay between such minor impurities, added reactive elements, and processing variables would therefore be important. A recognition of such an interplay has been absent in the past but would certainly be worthy of consideration in the future. Additional research is warranted in this area due to the increasing technological importance of oxidation resistant high temperature alloys.

V. FUTURE RESEARCH

Based upon the results of this study, efforts would be directed as follows:

1) the interrelationship between the indigenous sulfur present within the substrate alloy, the processes whereby protective aluminide coatings are formed and protective oxide scale adherence effects would be characterized.

2) the interrelationship between rapid solidification processing, added and indigenous elements, coating microstructure and composition would be characterized as such parameters influence the subsequent coating oxidation performance.

VI. ACKNOWLEDGEMENTS

The authors would wish to acknowledge Dr. B. Laube, Ms. C. Clark, Ms. J. Whitehead, and Mr. G. McCarthy all of UTRC for their assistance in Auger, scanning electron microprobe, scanning electron microscopy and scanning transmission electron microscopy analyses, respectively.

VII. REFERENCES

1. Whittle, D. P. and J. Stringer: Philos. Trans. R. Soc. London, Ser. Vol. A295, p. 309 (1980).

2. Tien, J. K. and F. S. Pettit: Metall. Trans. Vol. 3, pp. 1587-1599 (1972).

3. Antill, J. E. and K. A. Peakall: J. Iron Steel Inst. Vol. 205, pp. 1136-1142 (1967).

4. Golightly, F. A., F. H. Stott and G. C. Wood: Oxid. Met., Vol. 10, pp. 163-187 (1976).

5. Pfeiffer, H.: Werkst. Korros., Vol. 8, p. 574 (1957).

6. Smeggil, J. G., A. W. Funkenbusch and N. S. Bornstein: Thin Solid Films, Vol. 119, pp. 327-335 (1984).

7. Funkenbusch, A. W. and J. G. Smeggil: A Study of Adherent Oxide Formation, Annual Technical Report R83-916154-1, Office of Naval Research Contract N00014-82-C-0618 (October 1983).

8. Smeggil, J. G., A. W. Funkenbusch and N. S. Bornstein: "The Effect of Laser Surface Processing on the Oxidation Behavior of a Ni-Cr-Al-Hf Alloy", presented at the "Fourth International Conference on High Temperature and Energy Related Materials", sponsored by IUPAC at Sante Fe, New Mexico, April 2-6, 1984 and accepted for publication in High Temperature Science, currently in press.

9. White, C. L., J. H. Schneibel and R. A. Podgett: Metall. Trans., Vol. 14A, p. 425 (1980).

10. Chaung, H., J. G. Lunsden and R. A. Staehle: Metall. Trans., Vol. 10A., p. 185 (1974).

11. Mulford, R. A.: Metall. Trans., Vol. 14A, p. 865 (1983).

12. Doherty, J. E., A. F. Giamei and B. H. Kear: Can. Met. Quart., Vol. 13, p. 229 (1974).

13. Smeggil, J. G.: IEEE Trans. Mag. Vol. MAG-9, p. 168 (1973).

14. (a) Funkenbusch, A. W., J. G. Smeggil and N. S. Bornstein: Proposal for the Study of Adherent Oxide Scales. Technical Proposal (P83-19), Office of Naval Research Contract N00014-82-C-0618 (Jan. 1983).
(b) Smeggil, J. G., A. W. Funkenbusch and N. S. Bornstein: "Mechanistic Effect of Laser Surface Processing and Reactive Element Additions on the Oxidation Performance of Protective Coating Compositions". Presented at the Spring 1984 Electrochemical Society Meeting held in Cincinnati, OH.
(c) Funkenbusch, A. W., J. G. Smeggil and N. S. Bornstein: "Relative Element - Sulfur Interaction and Oxide Scale Adherence". Accepted for publication in Metall. Trans. (1985).

15. Luthra, K. L. and C. L. Briant: "AES Studies of the Surface Composition of FeCrAlY and NiCrAlY Alloys". Presented at the Spring 1984 Electrochemical Society Meeting held in Cincinnati, OH.

16. Gschneider, Jr., K. and N. Kippenhan: "THERMOCHEMISTRY OF THE RARE EARTH CARBIDES, NITRIDES AND SULFIDES FOR STEELMAKING", Report No. IS-RIC-5, (August 1971; Second Printing May 1972), Rare Earth Information Center, Institute for Atomic Research, Iowa State University, Ames Iowa 50010.

17. Hagar, J. P. and J. F. Elliott: Metal.Trans. Vol. 239, pp. 513-520 (1967).

18. Hansen, M.: "Constitution of Binary Alloys", McGraw-Hill Book Co., New York (1958).

19. Elliott, R. P.: "Constitution of Binary Alloys, First Supplement", McGraw-Hill Book Co., New York (1965).

20. Shunk, F. A.: "Constitution of Binary Alloys, Second Supplement", McGraw-Hill Book Co., New York (1969).

21. Moffett, W. G.: "Handbook of Binary Phase Diagrams", published by the General Electric Co., Corporate Research and Development Center, Schenectady, NY (1984).

22. Seah, M. P. and C. Lea: Phil. Mag., Vol. 31, p. 627 (1975).

23. Harris, L. A.: Journal of Applied Physics, Vol. 39, p. 1428 (1968).

24. Sickatua, E.: Surface Science, Vol. 19, p. 181 (1970).

25. Holloway, P. H. and J. R. Hudson: Surface Science, Vol. 33, p. 56 (1972).

26. Mroz, S., C. Kosiol and J. Kolaczkiewics: Vacuum, Vol. 26, p.61 (1975).

27. Burton, J. J., B. J. Berkowitz and R. D. Kane: Metall. Trans. Vol. 10A, p. 677 (1979).

28. Yoshihara, KI, M. Kurahushi and K. NII: Trans. Japan. Inst. Met. Vol. 21, p. 425 (1980).

FIGURE CAPTIONS

Fig. 1 Calculated surface concentration of sulfur vs. temperature for NiCrAl and NiCrAlY.

Fig. 2 Cyclic oxidation results (1050°C). Mass change vs. number of cycles.

Fig. 3 Cyclic oxidation results (1180°). Mass change vs. number of cycles.

Fig. 4 Non-metallic inclusions. NiCrAl Alloy As-Annealed.
A. Backscattered electron micrograph
B. X-ray map for aluminum
C. X-ray map for chromium
D. X-ray map for sulfur.

Fig. 5 Sulfur Enrichments in NiCrAl Alloy As-Annealed Back scattered electron micrograph. X-ray line scan for sulfur.

Fig. 6 Non-metallic Inclusions in NiCrAlY Alloy As-Annealed.
A. Backscattered electron micrograph
B. X-ray map for aluminum
C. X-ray map for chromium
D. X-ray map for yttrium
E. X-ray map for oxygen
F. X-ray map for sulfur.

Fig. 7 Yttrium Sulfide Particles in NiCrAl + Y_2S_3 As-Annealed.
A. Back scattered electron micrograph. X-ray line scan for yttrium.
B. Energy dispersive x-ray analysis of particles traversed by line scan in A. (Note: sulfur enrichment).

Fig. 8 Sulfur enrichment at scale-metal interface of undoped, vis a vis either Y_2S_3 or elemental yttrium additions, NiCrAl alloy isothermally oxidized at 1050°C for 100 hours. Back scattered electron micrograph. Line scan for sulfur across retained adherent oxide scale.
a. NiCrAl alloy
b. Retained oxide fragment.
c. Metallographic mounting material.

Fig. 9. Sulfur enrichments in particles at base of oxide scale removed from an undoped, vis a vis Y_2S_2, NiCrAlY alloy after 1050°C exposure for 100 hours.
A. Scanning transmission electron micrograph.
B. Energy dispersive x-ray analysis of particle identified in A. (Note: copper peak may be due to support grid.)

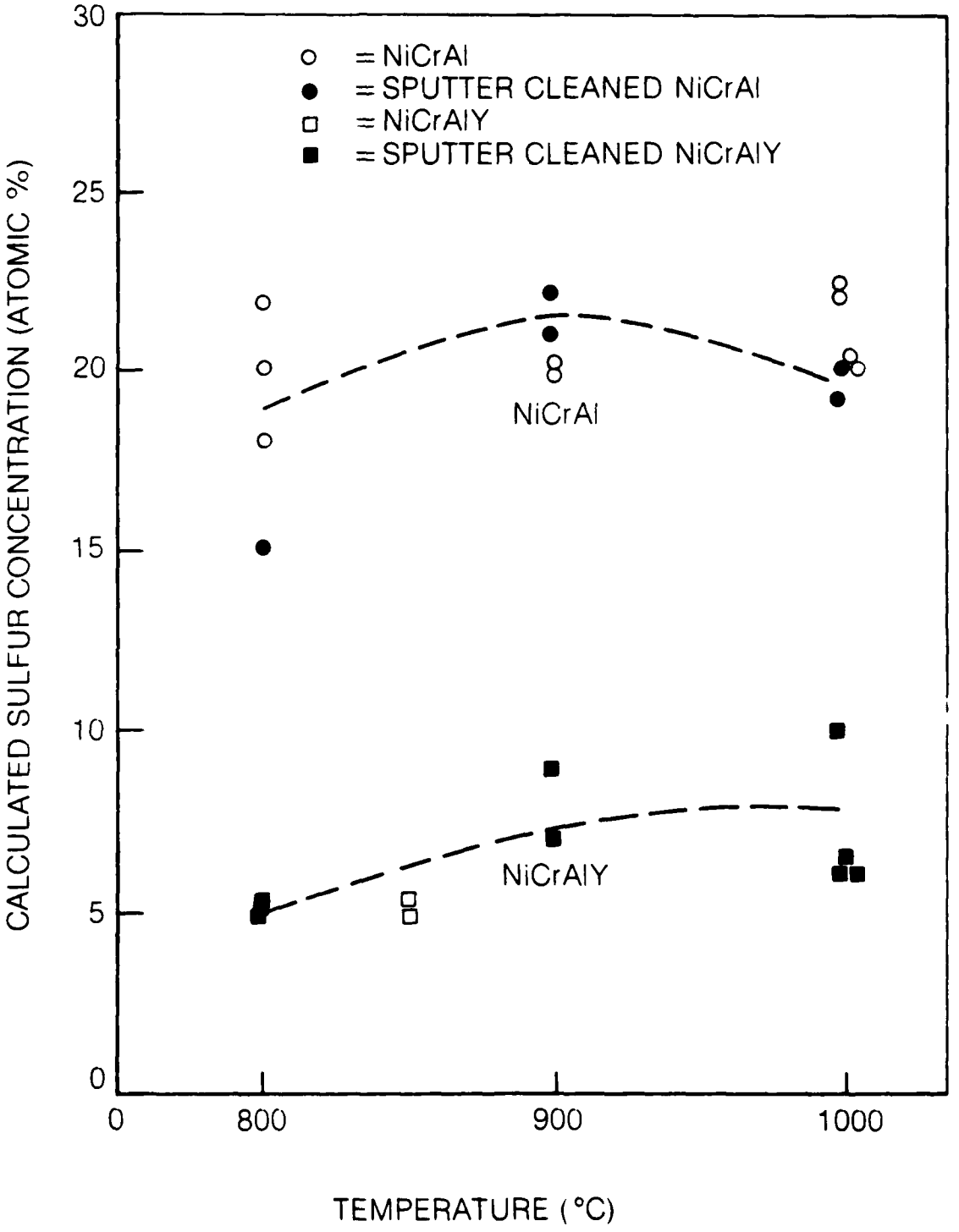

Figure 1 Calculated surface concentration of sulfur vs temperature for NiCrAl and NiCrAlY.

85-1-14-1

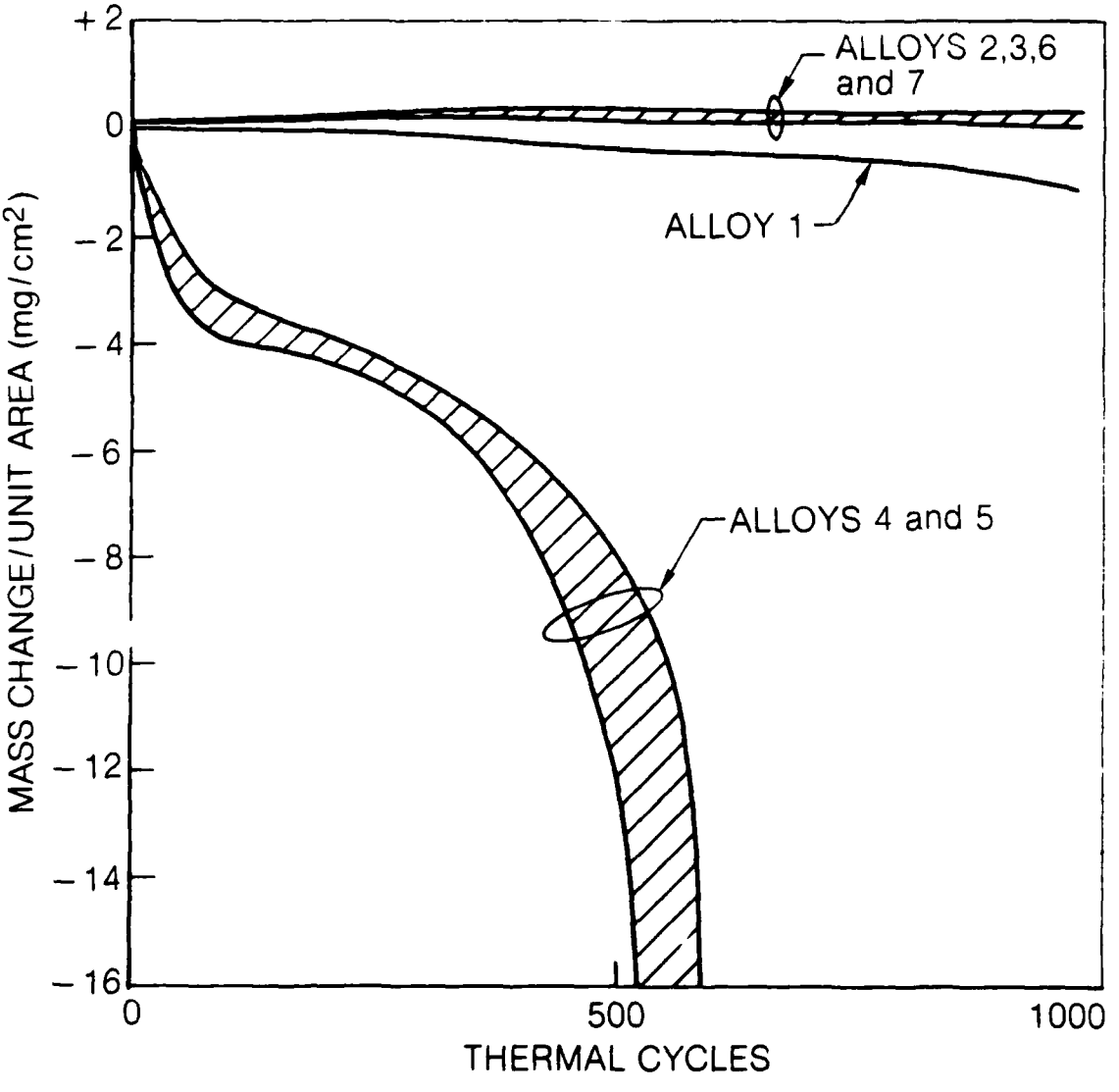

Figure 2 Cyclic oxidation results (1050 °C) mass change vs number of thermal cycles

84-7-97-3

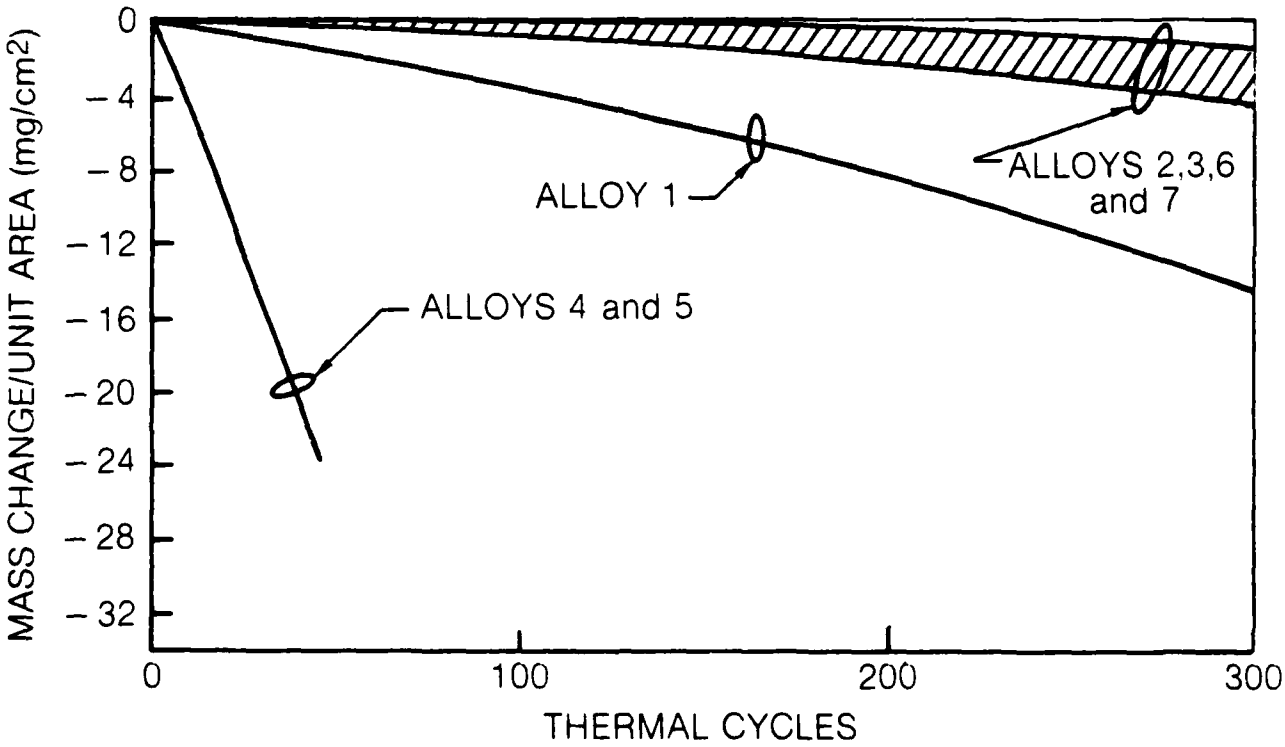

Figure 3 Cyclic oxidation results (1180 °C). Mass change vs. number of cycles.

85-2-48-1

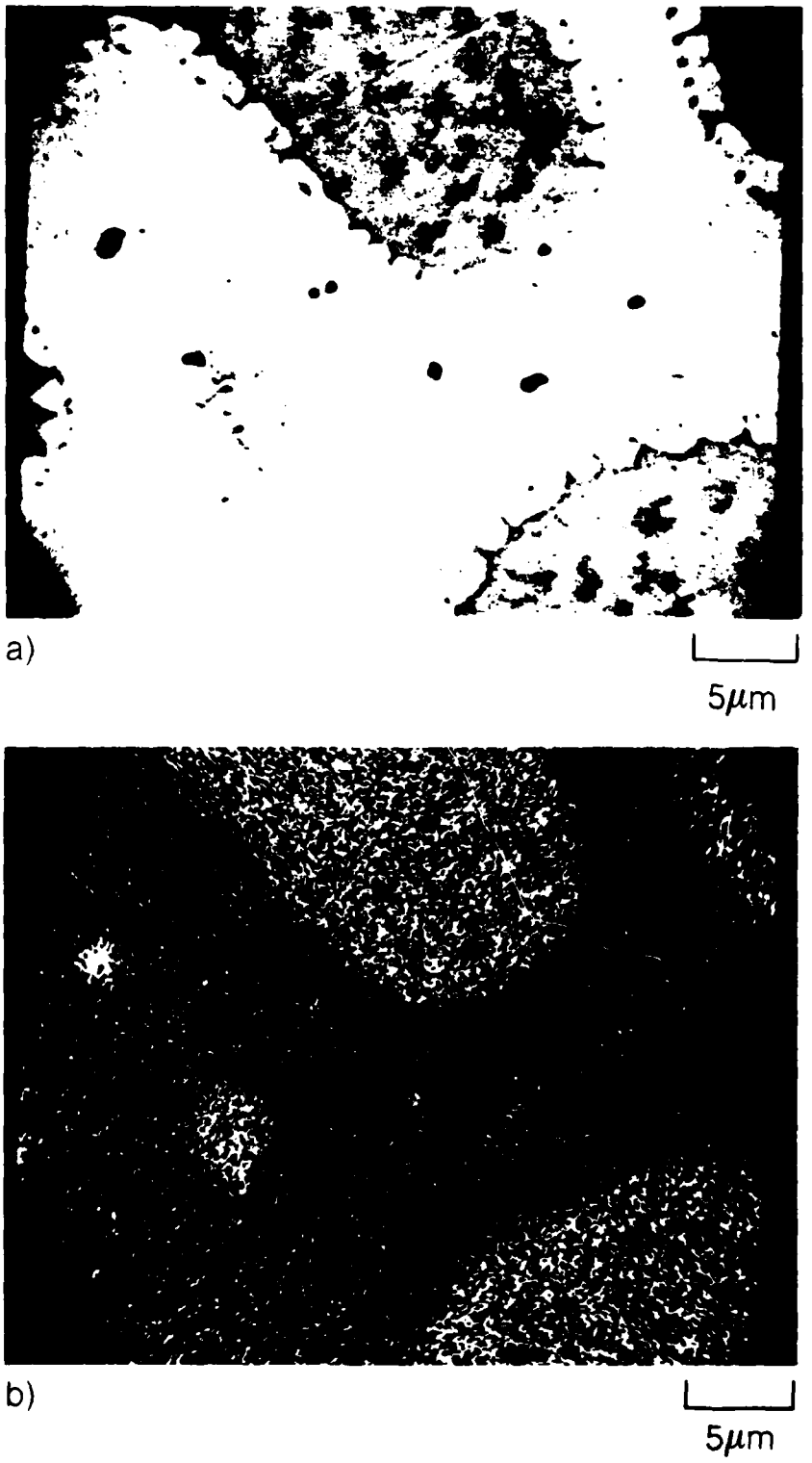

Figure 4 Non-metallic inclusions. NiCrAl alloy as-annealed.
a) Backscattered electron micrograph.
b) X-ray map for aluminum.

85-2-48-2

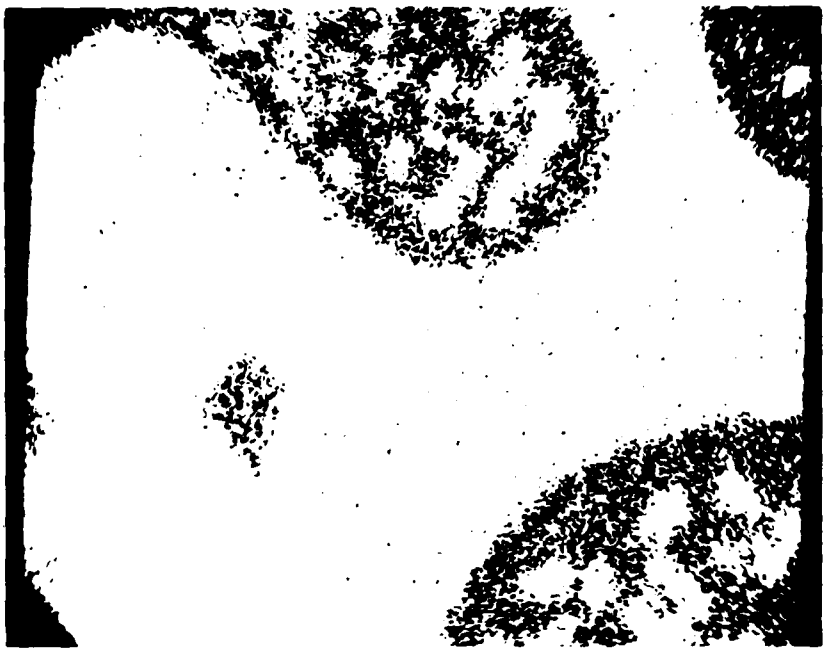

c)

5μm

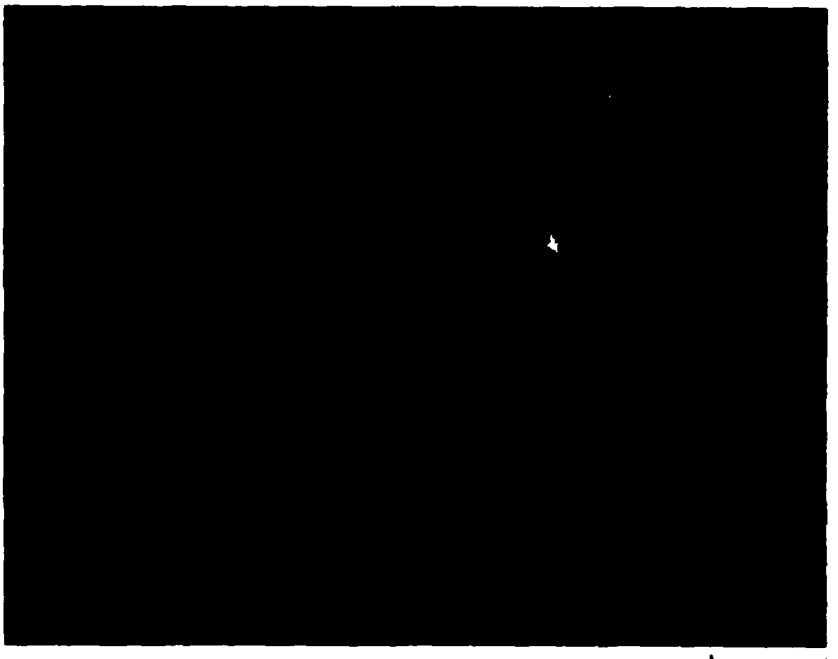

d)

5μm

Figure 4 Non-metallic inclusions. NiCrAl alloy as-annealed.
c) X-ray map for chromium.
d) X-ray map for sulfur.

85-2-48-3

Figure 5 Sulfur enrichments in NiCrAl alloy as-annealed.
Backscattered electron micrograph.
X-ray line scan for sulfur.

a)

7μm

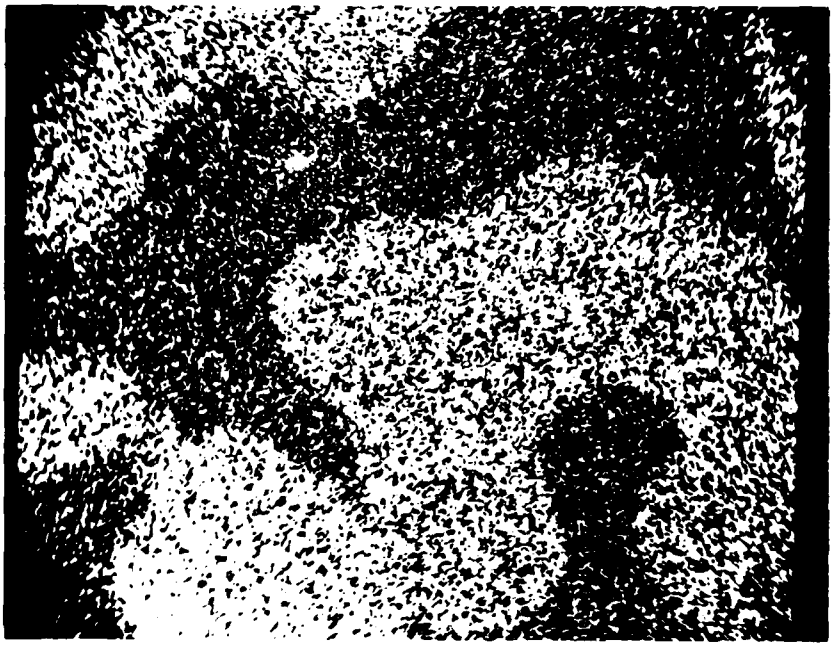

b)

7μm

Figure 6 Non-metallic inclusions in NiCrAlY alloy as-annealed.
a) Backscattered electron micrograph.
b) X-ray map for aluminum.

85-2-48-5

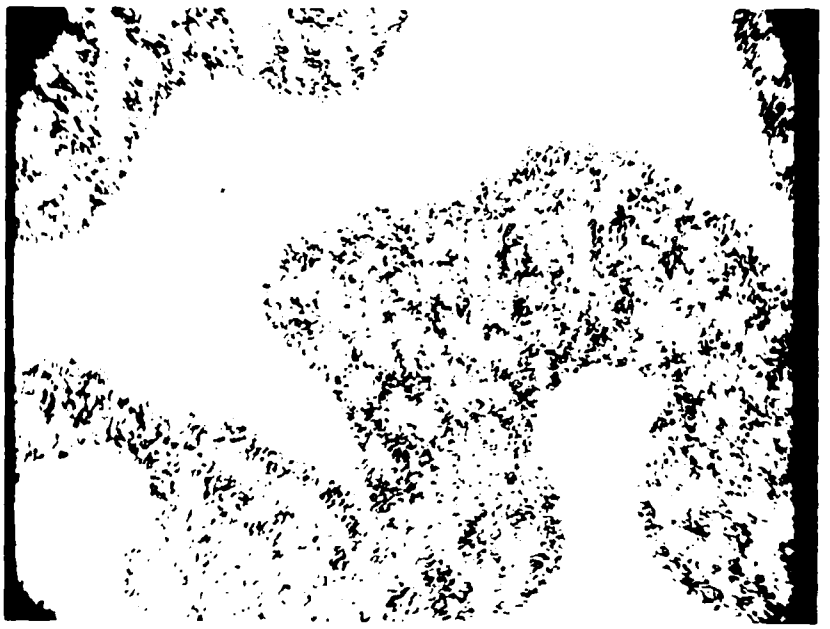

c)

7μm

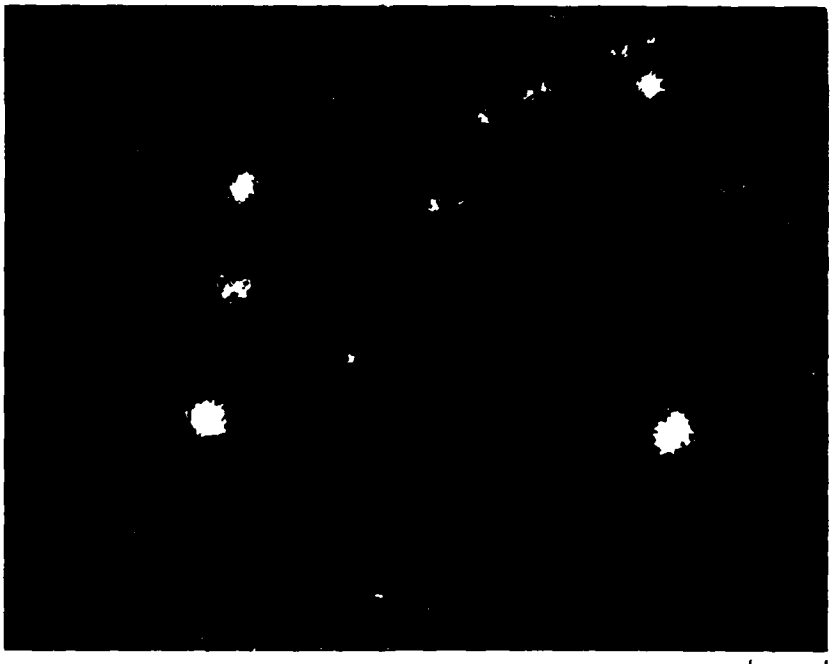

d)

7μm

Figure 6 Non-metallic inclusions in NiCrAlY alloy as-annealed.
c) X-ray map for chrominum.
d) X-ray map for yttrium.

85-2-48-6

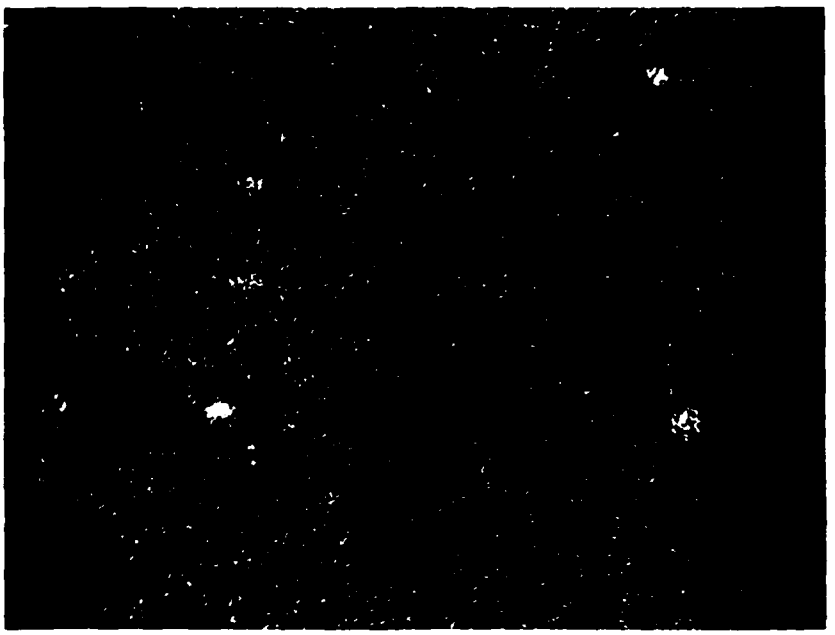

e)

7μm

f)

7μm

Figure 6 Non-metallic inclusions in NiCrAlY alloy as-annealed.
e) X-ray map for oxygen.
f) X-ray map for sulfur.

85-2-48-7

a)

4μm

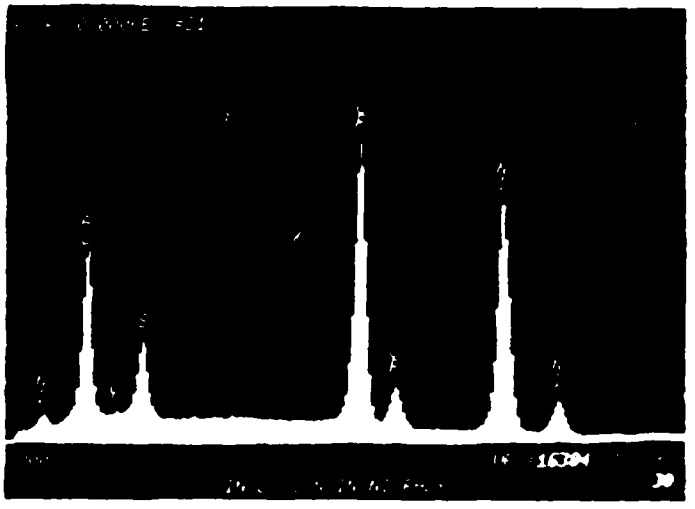

b)

4μm

Figure 7 Yttrium sulfide particles in NiCrAl + Y_2S_3 as-annealed.
a) Back scattered electron micrograph.
X-ray line scan for yttrium.
b) Energy dispersive x-ray analysis of particles traversed by line scan in A. (Note: sulfur enrichment).

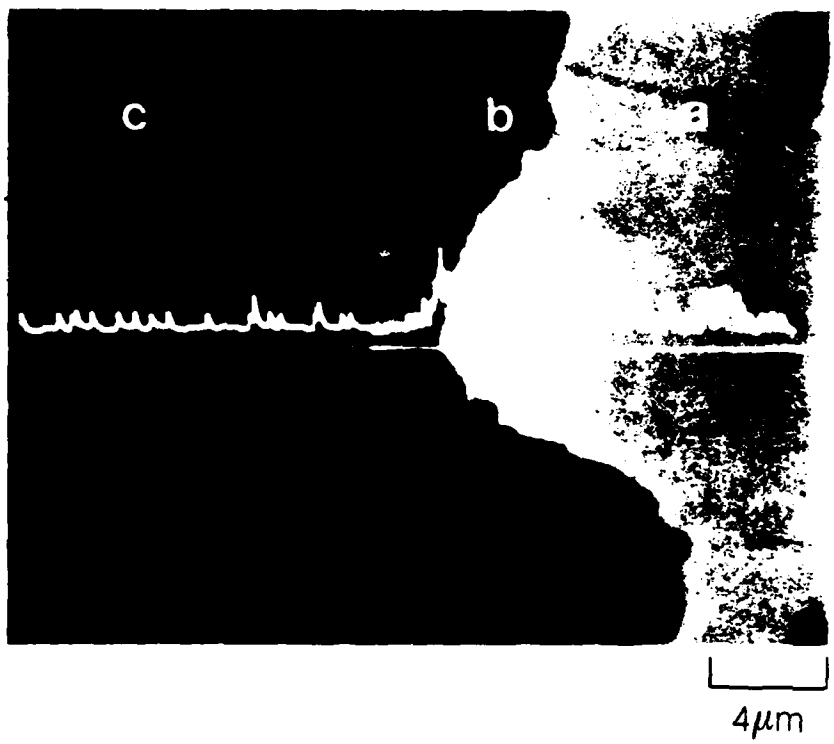

Figure 8 Sulfur enrichment at scale-metal interface of undoped, vis a vis either Y_2S_3 or elemental yttrium additions. NiCrAl alloy. Isothermally oxidized at 1050 °C for 100 hours. Back scattered electron micrograph. Line scan for sulfur across retained adherent oxide scale.
a) NiCrAl alloy.
b) Retained oxide fragment.
c) Metallographic mounting material.

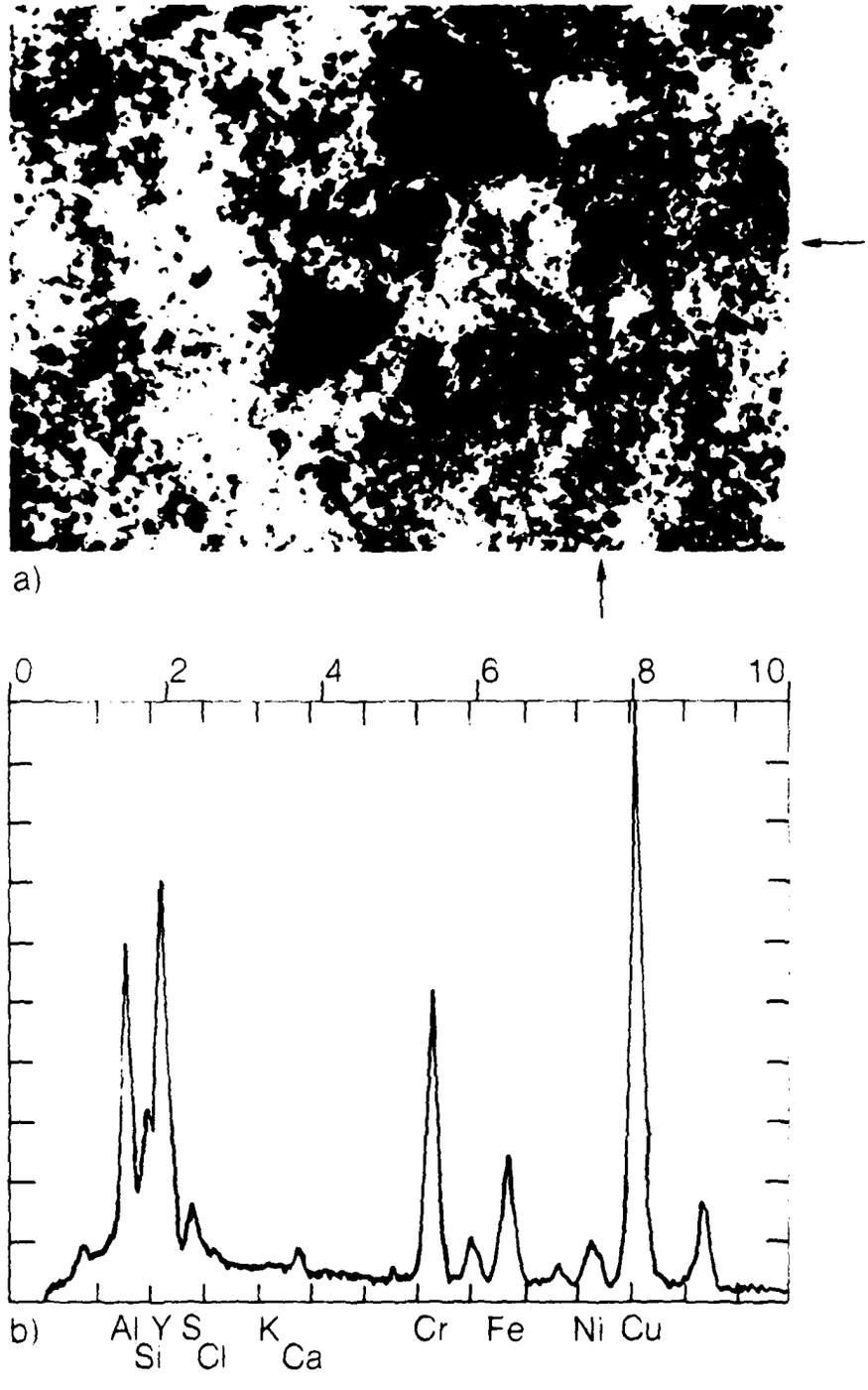

Figure 9 Sulfur enrichments in particles at base of oxide scale removed from an undoped, vis a vis Y_2S_3, NiCrAlY alloy. NiCrAlY after 1050 °C exposure for 100 hours.
a) Scanning transmission electron micrograph.
b) Energy dispersive x-ray analysis of particle identified in A. (Note: copper peak may be due to support grid.)

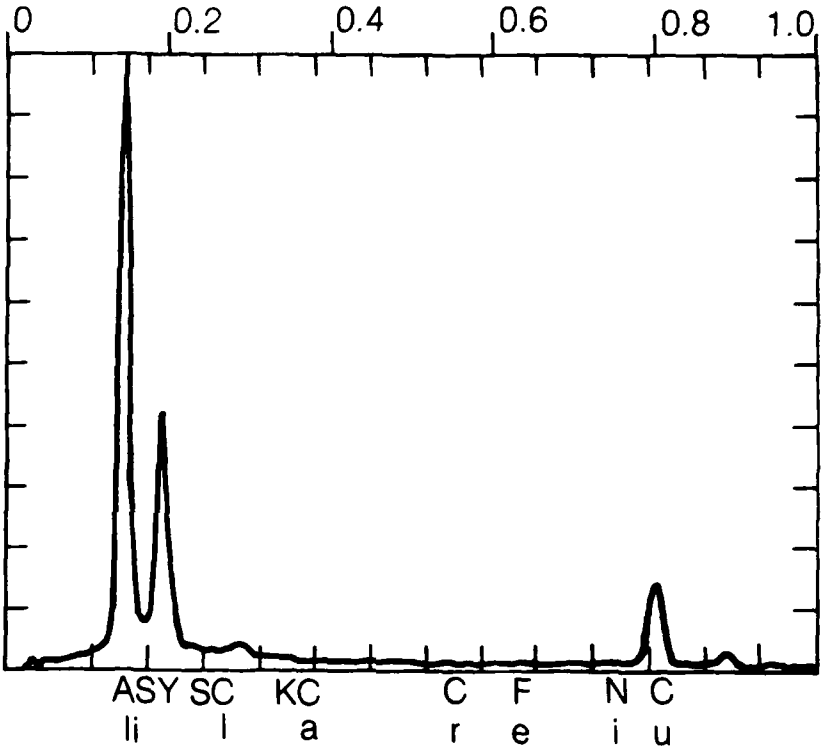

Figure 10 Sulfur-enrichments associated with yltria-containing particles at base of oxide scale from an undoped, vis a vis, laser surface processed NiCrAlY alloy.
a) NiCrAlY after 100 hours at 1050 °C
b) Energy dispersive x-ray analysis of typical particle at base of scale.

END

FILMED

7-85

DTIC